INDONESIAN JOURNAL ON GEOSCIENCE
Geological Agency
Ministry of Energy and Mineral Resources

Journal homepage: http://ijog.geologi.esdm.go.id
ISSN 2355-9314, e-ISSN 2355-9306

Petrogenesis of Rinjani Post-1257-Caldera-Forming-Eruption Lava Flows

Heryadi Rachmat[1,2], Mega Fatimah Rosana[1],
A. Djumarma Wirakusumah[3], and Gamma Abdul Jabbar[4]

[1]Faculty of Geology, Padjadjaran University
Jln. Raya Bandung - Sumedang Km. 21, Jatinangor, Sumedang, Indonesia
[2]Geological Agency
Jln. Diponegoro No. 57, Bandung, Indonesia
[3]Energy and Mineral Institute
Jln. Gajah Mada, Karangboyo, Cepu, Kabupaten Blora, Indonesia
[4]Hokkaido University, Kita 10, Nishi 8, Sapporo, Japan

Corresponding author: heryadirachmat220@gmail.com
Manuscript received: March 7, 2016; revised: May 17, 2016;
approved: June 29, 2016; available online: August 2, 2016

Abstract - After the catastrophic 1257 caldera-forming eruption, a new chapter of Old Rinjani volcanic activity began with the appearance of Rombongan and Barujari Volcanoes within the caldera. However, no published petrogenetic study focuses mainly on these products. The Rombongan eruption in 1944 and Barujari eruptions in pre-1944, 1966, 1994, 2004, and 2009 produced basaltic andesite pyroclastic materials and lava flows. A total of thirty-one samples were analyzed, including six samples for each period of eruption except from 2004 (only one sample). The samples were used for petrography, whole-rock geochemistry, and trace and rare earth element analyses. The Rombongan and Barujari lavas are composed of calc-alkaline and high K calc-alkaline porphyritic basaltic andesite. The magma shows narrow variation of SiO_2 content that implies small changes during its generation. The magma that formed Rombongan and Barujari lavas is island-arc alkaline basalt. Generally, data show that the rocks are enriched in Large Ion Lithophile Elements (LILE: K, Rb, Ba, Sr, and Ba) and depleted in High Field Strength Elements (HFSE: Y, Ti, and Nb) which are typically a suite from a subduction zone. The pattern shows a medium enrichment in Light REE and relatively depleted in Heavy REE. The processes are dominantly controlled by fractional crystallization and magma mixing. All of the Barujari and Rombongan lavas would have been produced by the same source of magma with little variation in composition caused by host rock filter process. New flux of magma would likely have occurred from pre-1944 until 2009 period that indicates slightly decrease and increase of SiO_2 content. The Rombongan and Barujari lava generations show an arc magma differentiation trend.

Keywords: post-caldera, lava, basaltic-andesite, fractional crystallization, magma mixing

How to cite this article:
Rachmat, H., Rosana, M.F., Wirakusumah, A.D., and Jabbar, G.A., 2016. Petrogenesis of Rinjani Post-1257-Caldera-Forming-Eruption Lava Flows. *Indonesian Journal on Geoscience*, 3 (2), p.107-126. DOI: 10.17014/ijog.3.2.107-126

Introduction

Rinjani volcano complex lies in Lombok Island, West Nusa Tenggara Province, Indonesia (Figure 1). The Lombok Island is tectonically located in the west of eastern most Sunda Arc where Australian Continental Plate subductes beneath Eurasian Plate. The crustal thickness is about 20 km (Curray *et al*., 1977). The Benioff-Wadati zone lies about 164 km beneath Rinjani (Nasution *et al*., 2010). The Rinjani calc-alkaline suite probably originated by partial melting of the peridotite mantle wedge overlying the active part of Benioff Zone beneath Lombok with

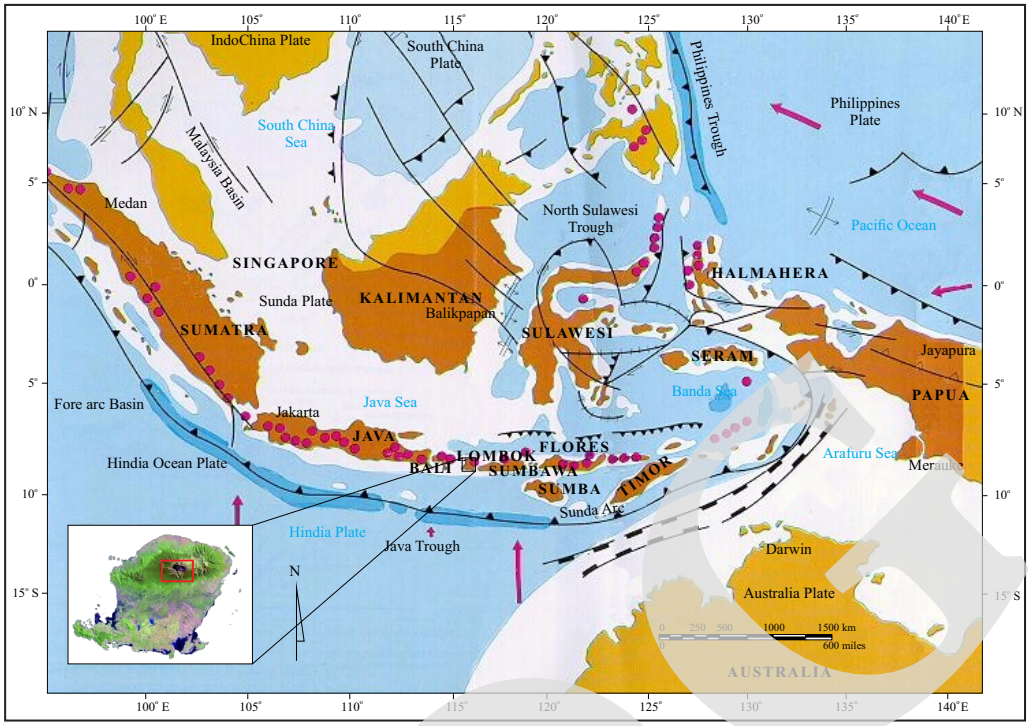

Figure 1. Map of Indonesia Archipelago and Lombok Island (the study area is indicated by the red square).

existence of variation in primary melts (Foden and Varne, 1981).

The aims of this paper is to discuss petrogenesis of lava from Rinjani post-caldera activity. The purpose of the paper is to complete our understanding of how Rinjani Volcano complex evolves, especially in post-caldera activity.

Geology of Lombok Island

Geologically, Lombok Island has been mapped by Mangga *et al*. (1994). Generally, the geological history of Lombok Island started from Tertiary (Early Miocene) until Holocene. Late Oligocene-Early Miocene Pengulung Formation is the oldest formation overlain by Middle Miocene Kawangan Formation. Both formations are intruded by Middle Miocene dacite and basalt that lead to the alteration of rock from those formations. Ekas Formations of Late Miocene in age overlies the previous older formations. Pengulung, Kawangan, and Ekas Formations form a hilly area in southern Lombok.

Lombok volcanic rock group overlies those older formations. This rock group comprises Kali Palung Formation which is a member of Selayar, Kalibalak, and Lekopiko overlying the older formation. The Lombok volcanic rock group is unconformably overlain by Quaternary Undifferentiated Volcanic Rock that presumably came from Pusuk, Nangi, and Rinjani Volcanoes. Alluvium appears as the youngest formation spreading around the shore.

Volcanic Activities of Rinjani Volcano Complex

The Rinjani Volcano activity can be divided into Pre-Stratocone Building stage, Stratocone Building stage, Low-Activity Stage, Syn-Caldera Stage, and Post-Caldera Stage (Nasution *et al*., 2004). The Pre-Stratocone Building stage leads to the formation of Old Rinjani or Samalas (Lavigne *et al*., 2013) that is much older than 12,000 years B.P.

The Stratocone Building stage produced Young Rinjani formed in the eastern flank of the Old Rinjani. Nasution *et al*. (2004) argued that the Stratocone Building stage had ages ranging from 11,940 ± 40 until 5990 ± 50 years B.P. The Low-Activity stage focused its activity in the Young Rinjani with the age of 2550±50 years B.P.

The Syn-Caldera stage relates to the catastrophic eruption that destroyed the Old Rinjani and led to the formation of the so-called Segara Anak Caldera. The tephra are pumice fall deposits, pumiceous pyroclastic-flow deposits, and debris-flow deposits. Nasution *et al*. (2004) argued that this catastrophic eruption occurred between AD 1210 and 1300 AD, whereas Lavigne *et al.* (2013) suggested that the eruption occurred between May and October 1257 AD, corresponding to the so-called "1258 mystery eruption" found in ice cores from both Greenland and Antarctica (Oppenheimer, 2003; Sigl *et al*., 2014, 2015). The products are mainly characterized by dacite with SiO_2 content ranges from 62 to 63 wt % (Nasution *et al*., 2004).

The catastrophic eruption in 1257 AD (Lavigne *et al*., 2013) led to the formation of a 6 km x 7 km caldera. This makes Rinjani one of great caldera-forming volcanoes in Indonesia. After this catastrophic caldera-forming eruption, there was an eruption from Young Rinjani that formed Segara Muncar Crater. Then, a new chapter of Rinjani volcanic activity began with the appearance of Rombongan and Barujari Volcanoes within the caldera (Rachmat, 2016) (Figures 2 and 3).

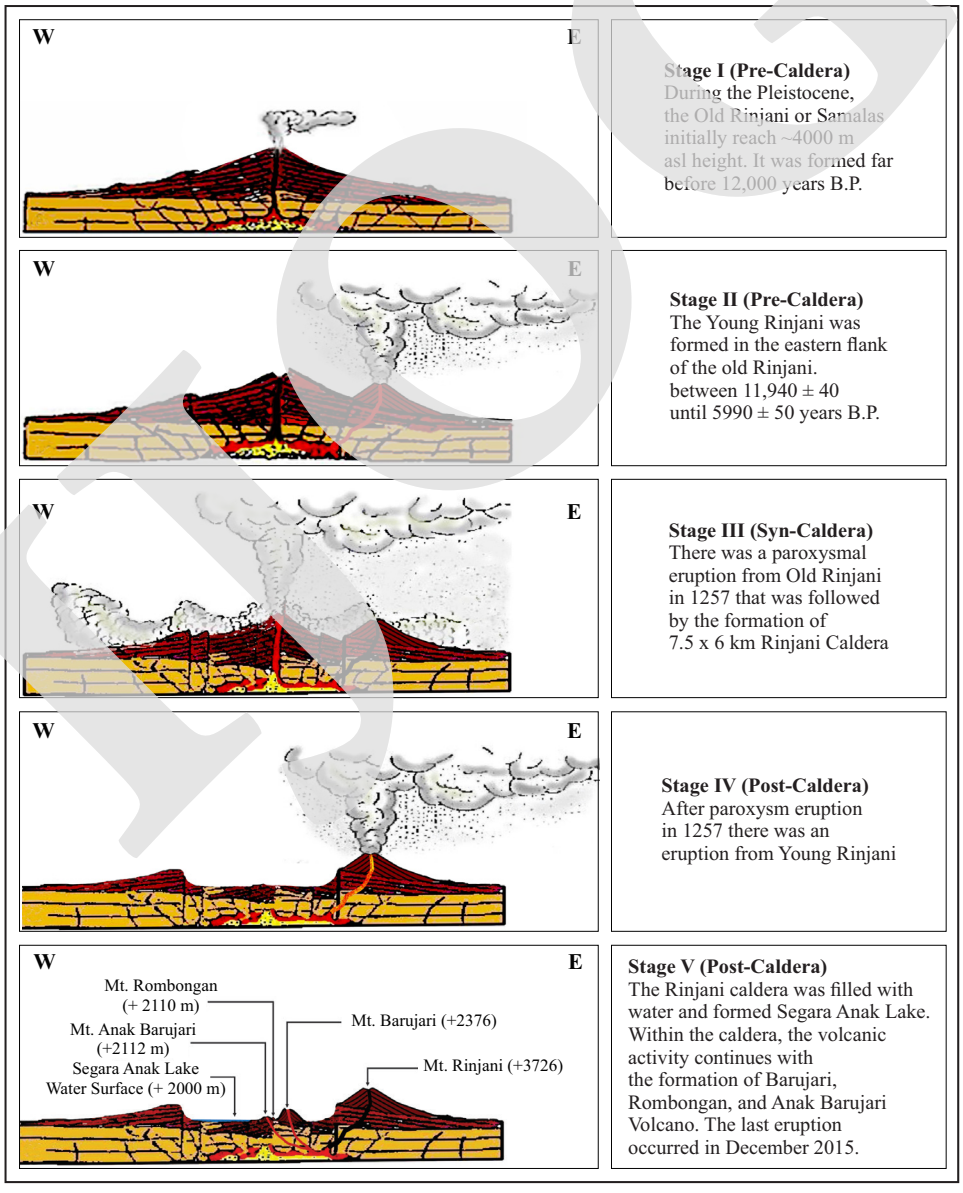

Figure 2. Evolution history of Rinjani Volcanic Complex (Rachmat, 2016; not to scale).

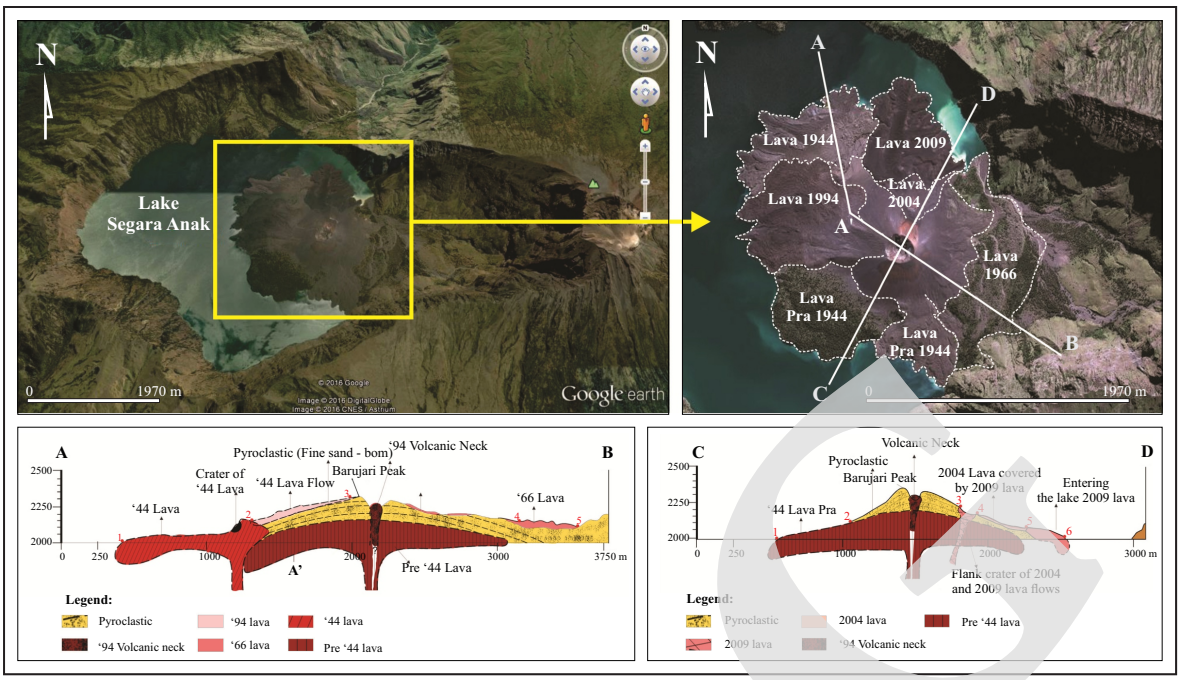

Figure 3. An aerial view of Rinjani Caldera (top image source: Google, left; CRISP, right)) and cross-section of Rombongan and Barujari Volcanoes (bottom, not to scale).

The Barujari concentrates the main post-caldera volcanic activity since the catastrophic event of 1257 AD. In 1944, the Rombongan Volcano appeared in the north of Barujari, but then its activity became extinct. Barujari erupted and spewed lava and scoria during its activities. The eruptions of Barujari Volcano consist of moderately explosive explosions and occasional lava flows (Komorowski *et al*., 2014). Barujari Volcano eruptions of 1884, 1904, 1906, 1909, and 1915 produced ash materials (Kusumadinata *et al.*, 1979).

The Rombongan eruption in 1944 and Barujari eruption in 1966, 1994, 2004, and 2009 produced basaltic andesite pyroclastic materials and lava flows (Rachmat and Iqbal, 2000; Nasution *et al.*, 2010).

A recent study on Rombongan and Barujari lava flows shows the characteristic of basaltic-andesitic lava (Komorowski *et al.*, 2014). The lava shows 53 - 55 wt.% of SiO_2 content, *i.e.* a less evolved magma than the syn-caldera forming products with 61 - 64 wt.% SiO_2 (Vidal *et al*., 2015). This less evolved characteristic of the Rombongan and Barujari lavas gives us information about the relatively true nature of magma source in this area.

Petrogenetic Study of Rinjani Complex

Hamilton (1974) discussed petrology and tectonic relationship in the Banda Arc Region. Volcanic rocks from the Banda arc islands are dominantly composed of mafic and intermediate calc-alkaline composition (andesite, basalt, and dacite) (Abbot and Chamalaun, 1981; van Bemmelen, 1949; Brouwer, 1942; Ehrat, 1928; Matrais, 1972; Neumann van Padang, 1951; Whitford *et al*., 1977). Rocks of the young volcanoes display an usual increase in the ratio of potassium to silicon with increasing distance to the Benioff zone beneath (Hatherton and Dickinson, 1969; Hutchison, 1976). Based on Foden and Varne (1980), the $^{87}Sr/^{86}Sr$ ratio from Rinjani is 0.70386 - 0.70402 and among the lowest in Sunda Arc. This low $^{87}Sr/^{86}Sr$ ratio suggests that the crust beneath Rinjani is also among the thinnest in the Sunda Arc.

Based on Foden and Varne (1980), Rinjani lava range varies from ankaramite and high-Al basalt to andesite and dacite. Futhermore, in 1981, Foden and Varne concluded that Rinjani

calc-alkaline suite probably originated by partial melting of the peridotite mantle wedge overlying the active Benioff Zone beneath the Lombok Island. However, they also notified the existence of some variations in primary melts that represent a separate evolving line. This is particularly the case for the ankaramite and high-Al basalt suite.

Based on whole-rock geochemistry, Nakagawa *et al*. (2015) grouped the rock into two folders: (1) stratovolcano building and post-caldera group, and (2) low-activity and caldera-forming group. Rocks from the stratovolcano building group mainly consists of basaltic andesite with SiO_2 ranging from 44.8 to 63.7%, while those from post-caldera group are olivine-pyroxene andesites (SiO_2 ~55%). This distinction is based on distinct chemical trends in the SiO_2 diagram for major and trace elements. The ratio of incompatible elements and Sr isotope are also distinct. Based on this this criterion, Nakagawa *et al*. (2015) suggested that the dacitic magma from low-activity and caldera-forming group could not be produced by a crystalization differentation of basaltic magma, but by additional processes, such as crustal melting and/or assimilation-fractional crystallization processes.

Moreover, Nakagawa *et al.* (2015) also suggested that the magma from low-activity stages was not the preceding stage of syn-caldera stage in term of petrogenesis. This argument is based on the difference in Sr isotope ratio and many chemical trends of magma from both stages.

Petrologic and geochemical studies of Rinjani Volcano had been conducted by many authors. Most of these studies mainly focused on the activities before and during the Syn-Caldera stage (*e.g.* Nakagawa *et al.,* 2015; Vidal *et al*., 2015). Another paper also discussed the petrogenetic in general term without correlation with Rinjani Activity stage (*e.g.* Foden and Varne, 1981). In this paper, petrogenesis of lava from Rinjani post-1257-caldera activity is mainly discussed.

The Rombongan and Barujari lava flows are a good subject for a petrogenetic study because:

1. There are no published research that focuses on these lava flows;
2. Relative clear information about lava flow time frame will give us a good temporal variation analysis;
3. A study of those lava flows will provide an understanding about magmatic evolution after the caldera-forming eruption.

Sampling and Methods

The Rombongan eruption in 1944 and Barujari eruption in pre-1944, 1966, 1994, 2004, and 2009 produced basaltic andesite pyroclastic materials and lava flows (Nasution *et al*., 2010). Only the lava products from each period of eruption are collected as samples for analyses. A total of thirty-one samples were analyzed and each period of eruption is composed of six samples except from 2004 with only one sample (Table 1).

The samples were used for petrography, whole-rock geochemistry, and Trace and Rare Earth Elements (REE) analyses (Table 1). The petrographic analysis was carried out using a Leica MPS 52 polarization microscope. The whole-rock geochemistry was determined at The Centre for Geological Survey (Geological Agency) Laboratory by X-ray fluorescence (XRF) analysis using ARL Advant XP+. Trace and Rare Earth Elements (REE) data were also determined at The Centre for Geological Survey (Geological Agency) Laboratory by Inductively Coupled Plasma-Mass Spectrometry (ICP-MS).

Result

Petrography

Most of lavas are porphyritic basalt to porphyritic andesite. The phenocrysts volume ranges from 39 % to 66 %. The dominant phenocrysts are plagioclase and pyroxene for all lavas. A small amount of K-feldspar was observed in all lavas except in 2004 and 2009 lavas. Groundmasses are dominantly composed of volcanic glass and plagioclase microlith. Opaque minerals were observed as groundmass in pre-1944 and 1944 lavas. Small amount of pyroxene microlith was

Table 1. Representatives of Whole-rock Geochemistry of Rinjani Post-caldera Lava (Manullang *et al.*, 2015)

Sample	Pre-1944 01	Pre-1944 02	Pre-1944 03	Pre-1944 04	Pre-1944 05	Pre-1944 06	1944 01	1944 02
wt%								
SiO_2	55.27	54.73	55.35	55.48	55.02	55.42	55.05	55.57
TiO_2	0.6	0.59	0.61	0.58	0.59	0.59	0.59	0.59
Al_2O_3	17.08	17.09	16.8	17.07	17.16	17.02	17.25	17.01
Fe_2O_3	2.92	3.01	3.01	2.89	2.92	2.86	2.90	2.93
FeO	6.12	6.31	6.31	6.06	6.13	6	6.10	6.16
MnO	0.17	0.17	0.17	0.61	0.17	0.17	0.17	0.16
MgO	3.19	3.09	3.5	3.3	3.24	3.25	3.01	3.09
CaO	9.04	9.63	8.69	8.68	9.2	9.01	9.26	8.68
Na_2O	3.13	3.02	3.2	3.27	3.11	3.13	3.12	3.25
K_2O	1.79	1.78	1.77	1.76	1.77	1.85	1.79	1.81
P_2O_5	0.2	0.19	0.19	0.91	0.19	0.19	0.19	0.21
Total	99.51	99.61	99.60	100.61	99.50	99.49	99.43	99.46
FeO*/MgO	2.74	2.92	2.58	2.62	2.70	2.64	2.89	2.85
Mg/Mg+Fe	-	-	-	-	-	-	38.10	38.50
Na_2O+K_2O	4.92	4.80	4.97	5.03	4.88	4.98	4.91	5.06
Fe*/(Fe*+Mg)								
ppm								
Rb	43.07	42.17	43.09	43.95	42.39	42.82	31.34	84.02
K	14860.58	14777.56	14694.54	14611.52	14694.54	15358.7	14860.58	15026.62
Th	4.88	4.45	4.59	5.95	4.61	5.65	4.02	3.85
Nb	4.79	6.15	5.7	7.89	3.56	2.53	2.17	
Ba	625.58	614.49	619.44	626.56	615.3	604.34	421.33	444.06
La	15.03	14.42	14.44	16.43	14.51	14.56	9.8	13.75
Ce	32.49	31.06	30.89	36.07	28.41	30.87	21.1	27.46
Sr	325.7	327.59	324.05	322.96	317.05	299.36	228.15	
P	872.84	829.2	829.2	3971.42	829.2	829.2	829.2	916.48
Ti	3597	3537.05	3656.95	3477.1	3537.05	3537.05	3537.05	3537.05
Y	23.37	23.1	23.41	24.05	22.69	22.47	16.77	19.71
V	181.52	201.36	189.17	196.79	171.41	153.61	144.18	256.6
Mn	1316.65	1316.65	1316.65	4724.45	1316.65	1316.65	1316.65	1239.2
Fe	61277.28	63175.54	63175.54	60667.84	61347.22	60058.4	61010.87	61620.31
Pr	3.86	3.37	3.37	3.94	3.77	3.67	2.41	3.58
Nd	14.96	14.59	14.73	15.22	14.68	14.19	9.33	13.9
Sm	3.66	3.6	3.62	3.71	3.62	3.41	2.32	3.39
Eu	1.19	1.19	1.17	1.19	1.18	1.11	0.76	1.06
Gd	3.95	3.88	3.78	4.06	3.82	3.7	2.52	3.68
Tb	0.68	0.67	0.67	0.7	0.66	0.65	0.43	0.63
Dy	3.87	3.83	3.81	4.06	3.79	3.71	2.43	3.47
Ho	0.87	0.86	0.86	0.9	0.85	0.84	0.53	0.79
Er	2.48	2.45	2.44	2.5	2.42	2.37	1.48	2.25
Tm	0.37	0.36	0.37	0.37	0.36	0.35	0.22	0.33
Yb	2.26	2.19	2.16	2.26	2.15	2.12	1.3	2

Table 1. ... continued

Sample	1944 03	1944 04	1944 05	1944 06	1966 01	1966 02	1966 03	1966 04
wt%								
SiO_2	55.59	55.22	55.18	56.16	56.06	55.15	56.44	56.4
TiO_2	0.58	0.6	0.59	0.57	0.56	0.59	0.57	0.58
Al_2O_3	17.01	16.88	17.17	17.15	17.11	17.18	17.07	16.96
Fe_2O_3	2.89	2.97	2.89	2.75	2.59	2.89	2.64	2.64
FeO	6.07	6.23	6.07	5.76	5.44	6.07	5.54	5.54
MnO	0.17	0.18	0.17	0.16	0.16	0.17	0.16	0.16
MgO	3.11	3.39	3.1	2.84	2.89	2.85	2.87	2.84
CaO	8.79	8.96	9.21	8.55	8.37	9.47	8.44	8.75
Na_2O	3.21	3.16	3.12	3.32	3.35	3.08	3.39	3.28
K_2O	1.84	1.79	1.78	1.88	1.95	1.84	1.96	1.99
P_2O_5	0.21	0.19	0.19	0.2	0.22	0.19	0.22	0.22
Total	99.47	99.57	99.47	99.34	98.70	99.48	99.30	99.36
FeO*/MgO	2.79	2.63	2.80	2.90	2.69	3.04	2.76	2.79
Mg/Mg+Fe	39.00	40.40	38.90	38.10	39.90	36.90	39.30	39.00
Na_2O+K_2O	5.05	4.95	4.90	5.20	5.30	4.92	5.35	5.27
Fe*/(Fe*+Mg)								
ppm								
Rb	83.1	82.75	86.46	83.18	76.04	97.34	104.58	100.33
K	15275.68	14860.58	14777.56	15607.76	16188.9	15275.68	16271.92	16520.98
Th	3.86	3.68	4.09	3.86	4.63	4.14	5.01	4.63
Nb			2.78		3.12	2.18	6.52	5.45
Ba	433.4	422.72	609.84	439.35	654.27	599.25	672.86	622.8
La	13.71	12.14	13.31	12.87	14.71	13.54	15.43	12.85
Ce	25.27	26.08	28.31	25.7	31.27	28.6	32.76	30.1
Sr			591.65		597.92	583.35	600.99	570.36
P	916.48	829.2	829.2	872.84	960.12	829.2	960.12	960.12
Ti	3477.1	3597	3537.05	3417.15	3357.2	3537.05	3417.15	3477.1
Y	19.38	20.8	22.08	21.82	23.05	21.94	23.42	19.84
V	250.29	257.37	162.39	403.11	143.96	155.19	180.38	146.07
Mn	1316.65	1394.1	1316.65	1239.2	1239.2	1316.65	1239.2	1239.2
Fe	60737.78	62362.96	60737.78	57683.9	54433.55	60737.78	55449.28	55449.28
Pr	3.55	3.42	3.48	3.7	3.81	3.51	3.88	3.65
Nd	13.86	13.38	13.6	14.08	14.75	13.53	15.11	14.1
Sm	3.37	3.25	3.33	3.44	3.54	3.33	3.65	3.41
Eu	1.07	1.01	1.13	1.05	1.17	1.12	1.22	1.15
Gd	3.63	3.5	3.66	3.64	3.82	3.62	3.96	3.68
Tb	0.63	0.61	0.64	0.62	0.67	0.63	0.69	0.64
Dy	3.43	3.29	3.66	3.44	3.71	3.59	3.88	3.62
Ho	0.78	0.75	0.81	0.78	0.84	0.8	0.87	0.81
Er	2.21	2.13	2.31	2.23	2.35	2.26	2.46	2.28
Tm	0.33	0.32	0.34	0.33	0.36	0.34	0.37	0.34
Yb	2.01	1.92	2.02	2	2.14	2.01	2.2	2.05

Table 1. ... continued

Sample	1966 05	1966 06	1994 01	1994 02	1994 03	1994 04	1994 05	1994 06
wt%								
SiO_2	55.74	58.88	55.03	55.09	55.21	54.95	55.29	55.94
TiO_2	0.57	0.54	0.62	0.62	0.6	0.6	0.6	0.57
Al_2O_3	17.12	16.63	16.9	16.73	16.9	17.11	16.96	17.15
Fe_2O_3	2.79	2.29	3.04	3.05	2.99	2.95	2.94	2.74
FeO	5.86	4.81	6.37	6.41	6.28	6.2	6.18	5.74
MnO	0.16	0.15	0.17	0.17	0.16	0.17	0.16	0.16
MgO	3.01	2.22	3.4	3.47	3.48	3.16	3.35	2.55
CaO	8.85	7.51	8.88	8.97	8.78	9.27	8.92	9.15
Na_2O	3.26	3.54	3.16	3.13	3.22	3.08	3.18	3.19
K_2O	1.84	2.33	1.77	1.8	1.73	1.81	1.75	1.97
P_2O_5	0.2	0.27	0.2	0.21	0.2	0.19	0.2	0.2
Total	99.40	99.17	99.54	99.65	99.55	99.49	99.53	99.36
FeO*/MgO	2.78	3.09	2.68	2.64	2.58	2.80	2.63	3.22
Mg/Mg+Fe	39.10	36.50	40.00	40.30	40.90	38.90	40.40	35.60
Na_2O+K_2O	5.10	5.87	4.93	4.93	4.95	4.89	4.93	5.16
Fe*/(Fe*+Mg)								
ppm								
Rb	111.2	80.38	111.96	115.4	75.22	76.22	103	76.95
K	15275.68	19343.66	14694.54	14943.6	14362.46	15026.62	14528.5	16354.94
Th	3.86	5.35	4.25	4.73	4.11	4.18	4.3	4.7
Nb	1.73	2.86	5.2	2.67	2.78	5.82	2.43	2.15
Ba	573.66	704.4	591.52	591.92	605.83	632.9	627.76	651.88
La	12.49	16.41	13.52	14.17	13.92	13.64	13.67	14.62
Ce	26.66	34.44	28.49	29.46	26.75	28.94	29.16	30.97
Sr	588.13	591.84	580.28	592.62	623.02	619.67	619.73	611.18
P	872.84	1178.33	872.84	916.48	872.84	829.2	872.84	872.84
Ti	3417.15	3237.3	3716.9	3716.9	3597	3597	3597	3417.15
Y	21.3	24.16	22.23	22.4	22.72	22.77	20.64	23.52
V	161.83	126	165.2	167.32	167.38	170.8	167.44	158.06
Mn	1239.2	1161.75	1316.65	1316.65	1239.2	1316.65	1239.2	1239.2
Fe	58636.37	48129.31	63784.98	64128.02	62839.19	62026.6	61823.46	57480.75
Pr	3.32	4.21	3.52	3.54	3.59	3.57	3.61	3.8
Nd	12.97	16.11	13.51	13.74	14.01	14.11	14.23	14.64
Sm	3.23	3.8	3.31	3.36	3.46	3.45	3.47	3.56
Eu	1.12	1.24	1.09	1.09	1.13	1.17	1.18	1.16
Gd	3.46	4.05	3.57	3.61	3.7	3.69	3.73	3.81
Tb	0.63	0.7	0.63	0.64	0.64	0.66	0.66	0.66
Dy	3.47	3.91	3.57	3.56	3.65	3.69	3.69	3.72
Ho	0.79	0.89	0.81	0.8	0.95	0.85	0.83	0.84
Er	2.18	2.49	2.25	2.26	2.28	2.35	2.78	2.4
Tm	0.34	0.39	0.34	0.34	0.34	0.36	0.36	0.36
Yb	1.92	2.29	2	1.99	2.01	2.08	2.07	2.12

Table 1. ... continued

Sample	2004 01	2009 01	2009 02	2009 03	2009 04	2009 05	2009 06
wt%							
SiO_2	55.74	58.88	55.03	55.09	55.21	54.95	55.29
TiO_2	0.57	0.54	0.62	0.62	0.6	0.6	0.6
Al_2O_3	17.12	16.63	16.9	16.73	16.9	17.11	16.96
Fe_2O_3	2.79	2.29	3.04	3.05	2.99	2.95	2.94
FeO	5.86	4.81	6.37	6.41	6.28	6.2	6.18
MnO	0.16	0.15	0.17	0.17	0.16	0.17	0.16
MgO	3.01	2.22	3.4	3.47	3.48	3.16	3.35
CaO	8.85	7.51	8.88	8.97	8.78	9.27	8.92
Na_2O	3.26	3.54	3.16	3.13	3.22	3.08	3.18
K_2O	1.84	2.33	1.77	1.8	1.73	1.81	1.75
P_2O_5	0.2	0.27	0.2	0.21	0.2	0.19	0.2
Total	99.40	99.17	99.54	99.65	99.55	99.49	99.53
FeO*/MgO	2.78	3.09	2.68	2.64	2.58	2.80	2.63
Mg/Mg+Fe	39.10	36.50	40.00	40.30	40.90	38.90	40.40
Na_2O+K_2O	5.10	5.87	4.93	4.93	4.95	4.89	4.93
Fe*/(Fe*+Mg)							
ppm							
Rb	111.2	80.38	111.96	115.4	75.22	76.22	103
K	15275.68	19343.66	14694.54	14943.6	14362.46	15026.62	14528.5
Th	3.86	5.35	4.25	4.73	4.11	4.18	4.3
Nb	1.73	2.86	5.2	2.67	2.78	5.82	2.43
Ba	573.66	704.4	591.52	591.92	605.83	632.9	627.76
La	12.49	16.41	13.52	14.17	13.92	13.64	13.67
Ce	26.66	34.44	28.49	29.46	26.75	28.94	29.16
Sr	588.13	591.84	580.28	592.62	623.02	619.67	619.73
P	872.84	1178.33	872.84	916.48	872.84	829.2	872.84
Ti	3417.15	3237.3	3716.9	3716.9	3597	3597	3597
Y	21.3	24.16	22.23	22.4	22.72	22.77	20.64
V	161.83	126	165.2	167.32	167.38	170.8	167.44
Mn	1239.2	1161.75	1316.65	1316.65	1239.2	1316.65	1239.2
Fe	58636.37	48129.31	63784.98	64128.02	62839.19	62026.6	61823.46
Pr	3.32	4.21	3.52	3.54	3.59	3.57	3.61
Nd	12.97	16.11	13.51	13.74	14.01	14.11	14.23
Sm	3.23	3.8	3.31	3.36	3.46	3.45	3.47
Eu	1.12	1.24	1.09	1.09	1.13	1.17	1.18
Gd	3.46	4.05	3.57	3.61	3.7	3.69	3.73
Tb	0.63	0.7	0.63	0.64	0.64	0.66	0.66
Dy	3.47	3.91	3.57	3.56	3.65	3.69	3.69
Ho	0.79	0.89	0.81	0.8	0.95	0.85	0.83
Er	2.18	2.49	2.25	2.26	2.28	2.35	2.78
Tm	0.34	0.39	0.34	0.34	0.34	0.36	0.36
Yb	1.92	2.29	2	1.99	2.01	2.08	2.07

also observed in 1966 and 1994 lavas. Textures that can be observed in all lavas are pyroxene inclusion in plagioclase, plagioclase inclusion in pyroxene, and glomeroporphyritic (Figure 4a). Sieve texture only appears in 1944 lava (Figure 4d) and 1966 lava (Figure 4f). Oscillatory zoned plagioclase is common in all lava except in Pre-1944 and 1944 lavas.

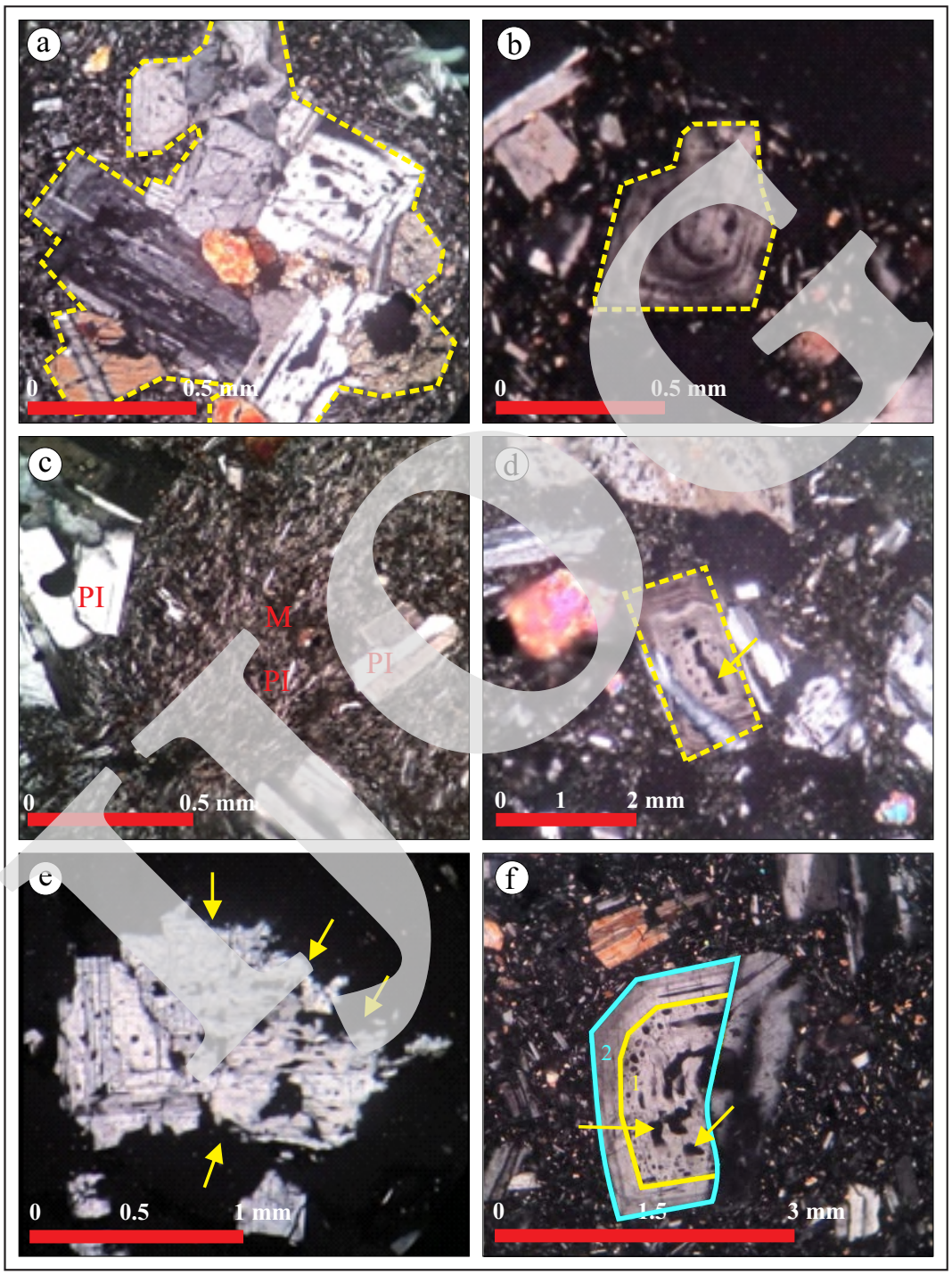

Figure 4. Photomicrographs of representative thin sections from: (a) 1966-5 lava that shows a glomeroporphyritic texture with plagioclase and pyroxene accumulate, (b) 2009-6 that shows an oscillatory zoning in plagioclase, (c) 2004-1 lava showing a pilotaxitic texture indicating flow mechanism during the generation of the lava, (d) 1966-2 that shows plagioclase with a sieve texture, (e) resorbed plagiocase from 1966-1 sample, and (f) plagioclase with a sieve texture that coated by euhedral plagioclase, from 1994-6 lava sample (Manullang *et al.* 2015).

Geochemistry

Results of whole-rock geochemistry analysis comprising major-, trace-, and rare-earth elements (REE) of Rinjani Post-caldera Lava are presented on Table 1.

Major Elements

The dominant element is SiO_2 having a high amount in a very narrow range (54.73 - 58.8 wt.%), followed by a relatively high Al_2O_3 concentration (>16 wt.%), whilst MgO shows a low content (<3.6 wt.%) (Table 1).

On the basis of data plotted on the Le Bass diagram, products of Rinjani (Barujari and Rombongan Volcanoes) post-1257 caldera eruption are dominantly composed of basaltic-andesite type, except sample-1966 lava having an andesitic composition (Figure 5). Furthermore, by plotting the data on Peccerillo and Taylor diagram (1976) (Figure 6), the rocks tend to fall under high K calc-alkaline affinity with minor calc-alkaline one. Therefore, the volcanic products of Rinjani can be classified as high K calc-alkaline to calc-alkaline basaltic-andesite type.

The Harker variation diagram for major elements shown in Figure 7 a and c indicates positive relationships that increases in SiO_2 content tend to be associated with increases in K_2O and Na_2O

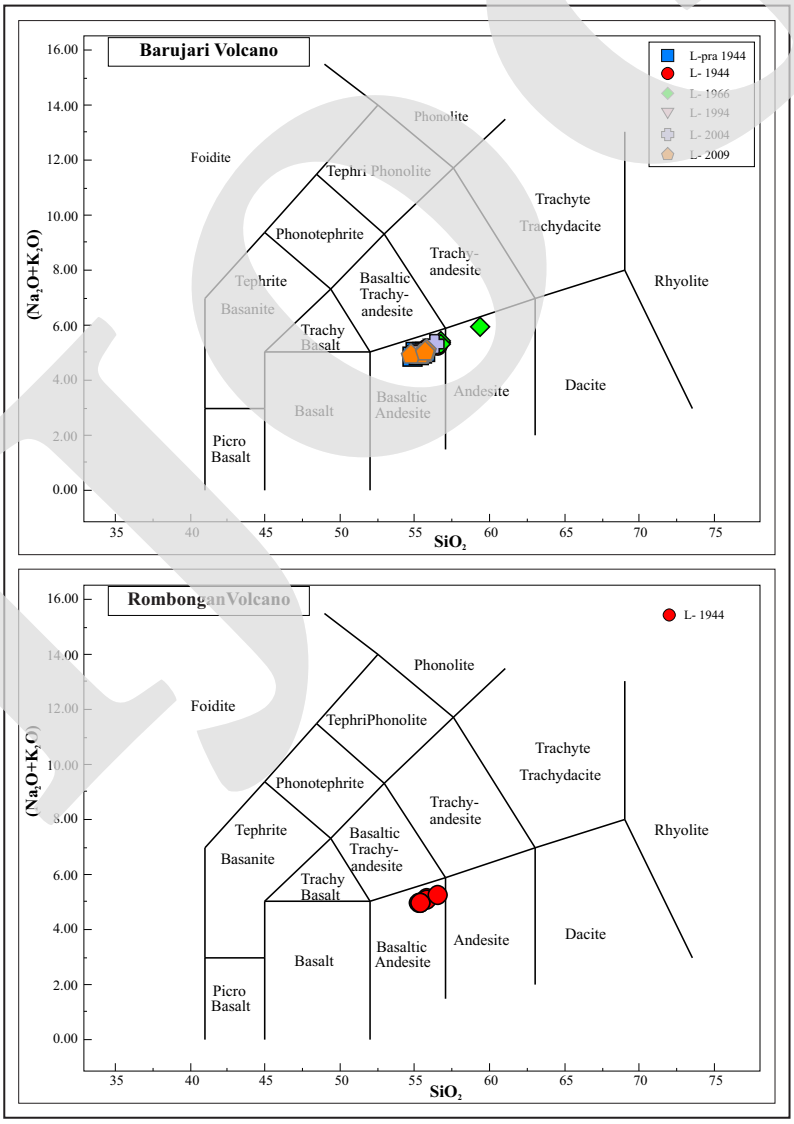

Figure 5. Plotting total alkali silica (Na_2O+K_2O) *vs*. SiO_2 using Le Bass diagram (Le Bass, 1986; Rollinson, 1993; Manullang *et al*., 2015) showing rock classification of the Rombongan and Barujari Volcanoes.

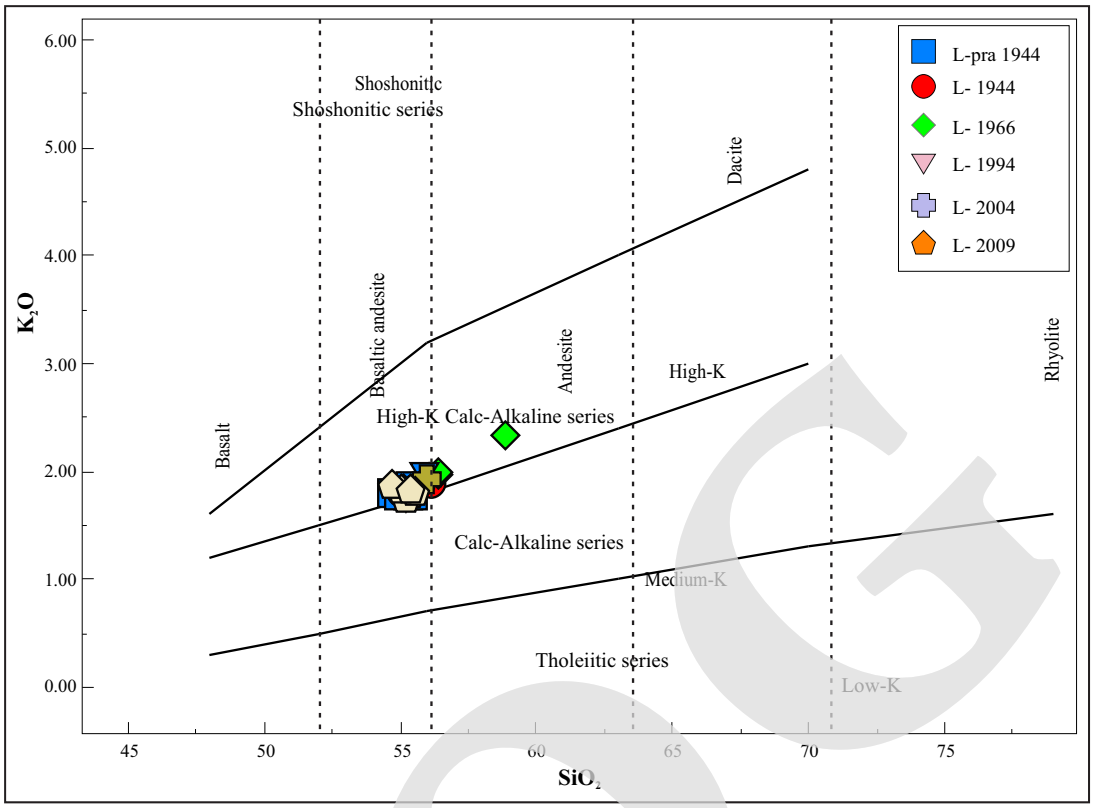

Figure 6. Rock affinity based on plotting K_2O *vs.* SiO_2 of Peccerillo and Taylor (1976) and Manullang *et al.* (2015).

contents. On the contrary, increases of SiO_2 values are associated with decreasing amounts of MgO, Fe_2O_3, TiO_2, Al_2O_3, and CaO, as shown in Figures 7b, c, d, f, and g, respectively, displaying negative correlations. Furthermore, Figures 7d and 7f indicate weak negative correlations. Additionally, an almost no-apparent relationship occurs between SiO_2 and P_2O5 (Figure 7h) as well as SiO_2 *vs.* MnO (Figure 7i).

The sample which shows a notable value is Lava 1966-06, displaying very high SiO_2 content (>58.88 wt.%) relative to the others. This value is also supported by the trace and rare earth elements values, which are also relatively high in the same samples.

Trace Elements

The trace element data were plotted into a spider diagram using Wood's chondrite normalization (Figure 8). Generally, data show that the rocks are enriched in Large Ion Lithophile Elements (LILE: K, Rb, Ba, Sr, and Ba) and depleted in High Field Strength Elements (HFSE: Y, Ti, and Nb) which is a typical suite from the subduction zone. Nb and P display steeply depleted values that show relatively nearly similar with Nb and P values from Mid Oceanic Ridge Basalt (MORB) and Oceanic Island Basalt (OIB).

Rare Earth Elements

REE were plotted into a spider diagram with Haskin chondrite normalization (Figure 9). Lavas from all periods show a relatively similar pattern. The pattern displays an enrichment in Light REE and relatively depleted in Heavy REE. Value of (La/Yb) N is between 3 and 4, which suggests a medium enrichment in Light REE. Sample of lava 2009-2 shows high Nm with 0.58 ppm, that is easily recognized in the REE pattern.

All of the samples show enrichment of Rb, K, Th, Ba, La, Ce, and Sr relative to those from Mid-Oceanic Ridge Basalt. The trend indicates a similar pattern with those from Oceanic Island Basalt and Upper Crust, but several elements relatively depleted, such as Nb (Figure 9).

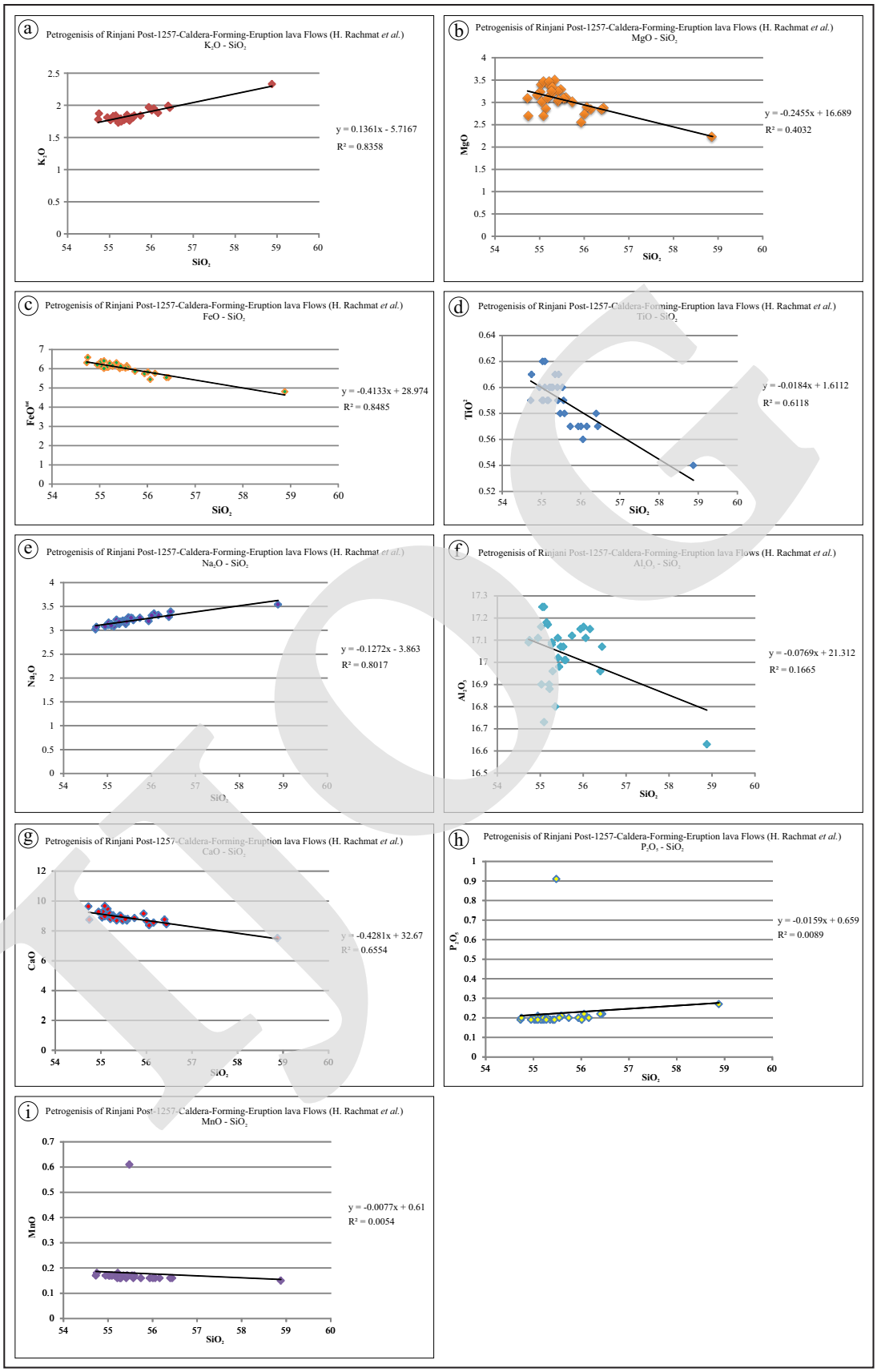

Figure 7. Harker variation diagram of SiO_2 *vs*. other oxides (a. K_2O; b. MgO; c. FeO^{tot}; d. TiO_2; e. Na_2O; f. Al_2O_3; g. CaO; h. P_2O_5; and i. MnO) of pre-1944 lava - 2009-lava (Manullang *et al.*, 2015).

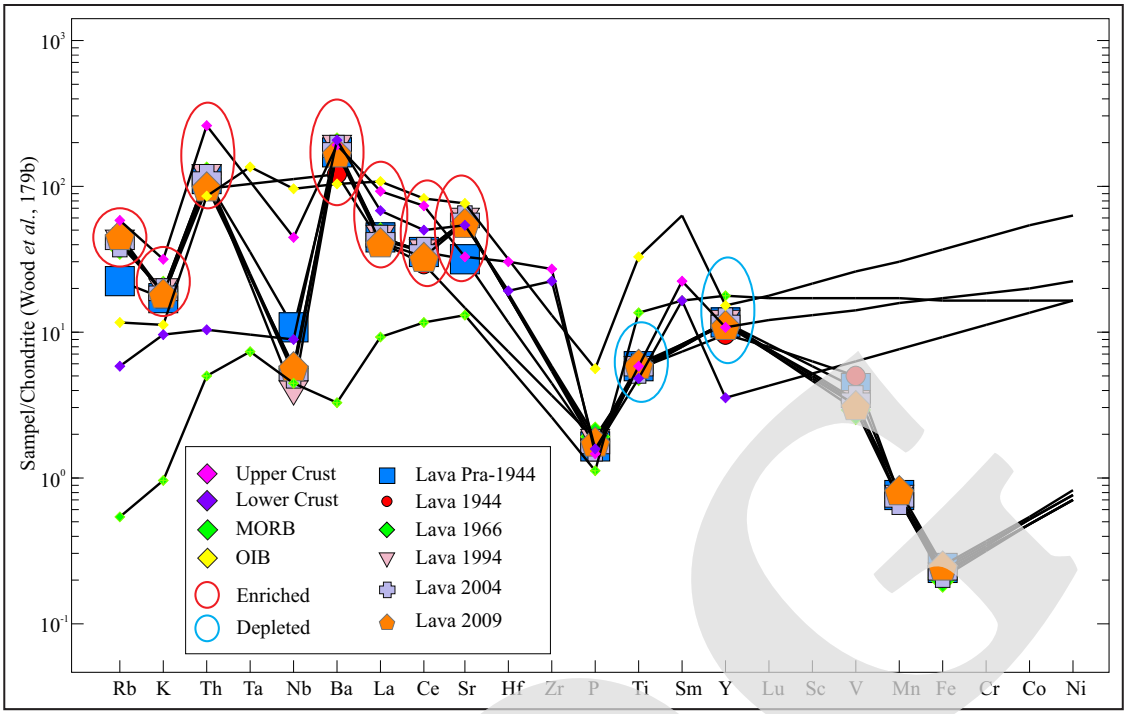

Figure 8. A spider diagram showing trace element variation of Rinjani 1257 post-caldera lava (normalized to chondrite).

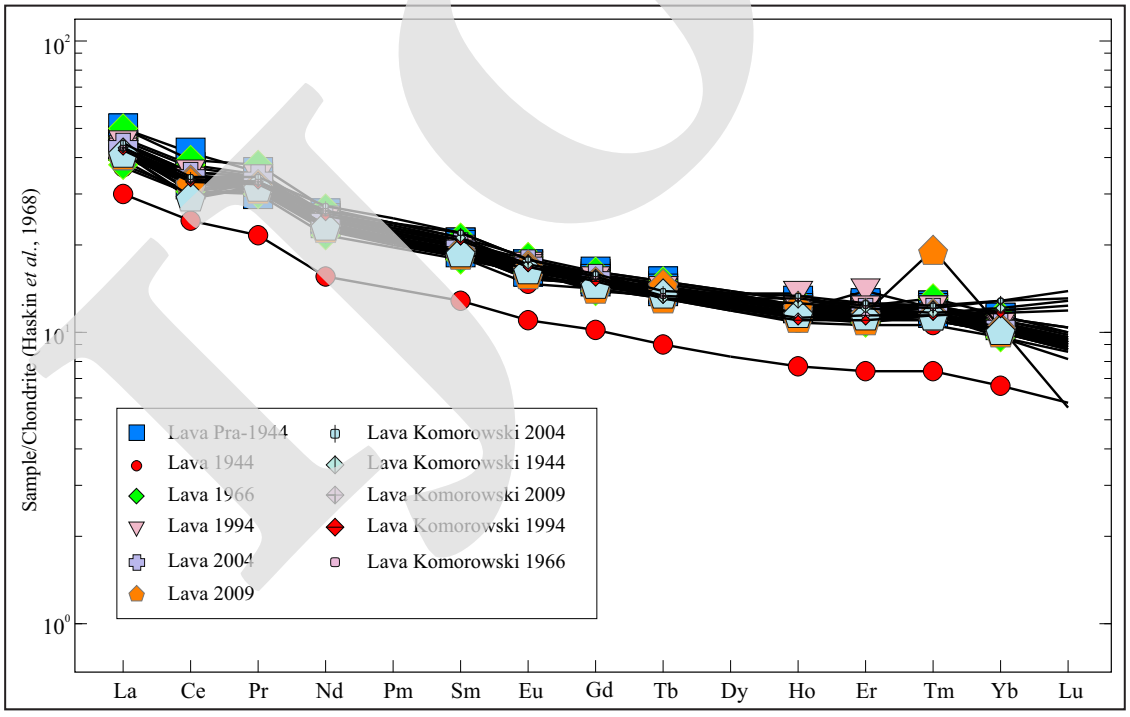

Figure 9. A spider diagram showing rare earth element (REE) variation of Rinjani 1257 post-caldera lava (normalized to chondrite).

Value of (Eu/Eu*) is 0.9, relating to a very low negative Eu anomaly. Hanson (1980) argued that the presence of feldspar would contribute to negative Eu anomaly in the melt, whereas the presence of pyroxene would contribute to positive Eu anomaly. This very low negative Eu

anomaly is possible because of the co-presence of plagioclase and pyroxene during the melting processes or the minimum presence of both plagioclase and pyroxene.

Discussion

Magma Mixing

Magma mixing is likely to have occurred during the generation of Barujari Lava. It can be demonstrated by the appearance of sieve texture, oscillatory zoned plagioclase, and resorption texture. The sieve texture is interpreted by some authors as the result of a mixing process (*e.g.* Nixon and Pearce, 1987).

The sieve texture coated by a relatively euhedral plagioclase can be found in 1994-6 lava (Figures 4b, 4d, 4f). The sieve texture is likely formed, at first as a consequence of mixing of two batches magma with different composition. As the crystallization continues after the mixing process, the growth of plagioclase also continued and coated the sieve-textured plagioclase.

The oscillatory zone plagioclase can be found in several samples (*e.g.* lava 1966-2, 2004-1, 2009-6). Oscillatory zoning usually occurs because of dynamic conditions of crystallization that lead to compositional changes. Another effect of new magma injection is, as stated before, resorption of already crystallized mineral in the magma chamber. The repeated injection of fresh basic magma into the chamber of differentiated magma could cause resorption of already crystallized plagioclase (Nixon and Pearce, 1987). The resorption texture can be found in 1966-1 lava where a plagioclase crystal was likely corroded by a hot magma.

The magma mixing process could also be implied by temporal variation within Barujari and Rombongan lavas. The MgO versus SiO_2 diagram shows that pre-1944 and 1994 lavas could possibly be a basic end-member and 1966 lava is the highest silica end-member. The 1944 lava lies between the two end members and could be a transition product. After the forming of the pre-1944 lava, it evolved to more silicic condition and produced basaltic andesite end-member lava (1944 and 1966). The 1994 lava is compositionally more basic and relatively similar to the pre-1944 lava. It could be an indication of new supply of magma after 1966 eruption that led to the formation of more basic 1994 lava.

Fractional Crystallization

Evidences of the occurrence of fractional crystallization process can be obtained from SiO_2 variation diagram and trace elements trend. Frost and Frost (2014) argued that suite of rocks related by fractional crystallization will form curved arrays, whereas those that related by magma mixing will form linear trend on the Harker diagram. The Harker diagram of TiO_2 and CaO versus SiO_2 of Rinjani post-caldera lava form curved arrays (Figure 6). Therefore, it suggests that the fractional crystallization process likely occurred in the genesis of Rinjani post-caldera lava.

The relatively low Mg number (100*Mg/Mg+Fe) (Table 1) suggested that lava from Barujari and Rombongan Volcanoes had undergone extensive modification (*e.g.* 1966-6 lava : Mg number 1966-1 = 0.18; 1966-2 = 0.16; 1966-5 = 0.17; 1966-6 = 0.16). These Mg numbers were lower than 0.28 which means the magma was not originated from the mantle. This argument is similar with the argument of Annen *et al*. (2006). This argument is also supported by Foden and Varne (1981) who argued that low Mg/Mg+Fe values and low Ni concentrations of many members of the Rinjani suite, particularly andesites and dacites, suggested that the mantle derived melts must have undergone an extensive modification as a result of fractional crystallization. Normal plagioclase zonings that occur in many basaltic andesitic of Barujari and Rombongan lavas also support the fractional crystallization processes.

Differentiational Trend

Frost and Frost (2014) argued that tholeiitic basalt and island-arc environment were similar in terms of major element composition, but they

followed different differentiation trends. This can be illustrated using a plot of $Fe^{tot}/(Fe^{tot}+Mg)$ versus SiO_2 (Figure 10).

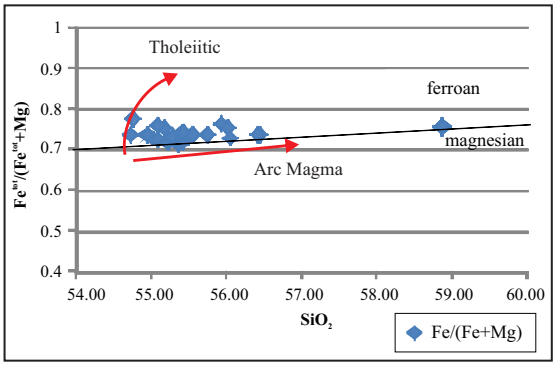

Figure 10. $Fe^{tot}/(Fe^{tot}+Mg)$ *vs*. SiO_2 diagram that shows arc magma differentiation trends (after Frost and Frost, 2014).

During differentiation, tholeiitic melts from oceanic environment become enriched in Fe relatives to Mg. This ferromagnesian silicates in the lavas become enriched in iron end member as differentiation progresses and late in the differentiation history the melts underwent silica enrichment. In contrast, arc magma suites show a strong enrichment in silica with increasing differentiation but ferromagnesian silicates show moderately increases in the Fe/(Fe+Mg) ratio. From this plot, it can be concluded that the Rombongan and Barujari lavas underwent an arc character differentiation where moderate ferromagnesian increase occurs.

The trend also implies that the differentiation trend moves toward the magnesian field. It implies that iron enrichment was inhibited during the earlier stage of differentiation due to early crystallization of Fe-Ti oxides. This kind of differentiation trend leads to the presence of magnesian-rich pyroxene end member, such as diopside and hypherstene, in highest silica-end member rocks (*e.g.*1966 lava) in CIPW norm calculation (Table 2).

Magma Source

Hartono (1997) argued that petrogenetic models for andesite genesis fell into several categories, those are: 1) crust-level fractional crystallization of primary basaltic magma from partial melting of mantle peridote, 2) fractional crystallization of basaltic precursors accompanied by assimilation of crustal rocks, 3) mixing of basalt and melted sialic crust, 4) lower crustal melting, assimilation, storage, and homogenization, and 5) partial melting of subducted oceanic lithosphere.

Trace elements patterns from all of the samples show a similar pattern. This would likely imply that the Barujari and Rombongan lavas were derived from the same source of magma. Very low (Eu/Eu*) anomaly (0.9) and the appearance of plagioclase and pyroxene in most of the samples would suggest that the magma have undergone plagioclase and pyroxene fractionation.

Partial melting of subducted oceanic lithosphere model would likely be impossible because of the relatively low contents of Mg-number (<0.28). Annen *et al.* (2006) also argued that arc andesite with low Mg-number could not have been in a direct equilibrium with the mantle. Therefore, other processes would be involved during magma ascending.

High concentration of Al_2O_3 (>16 wt %) and high content of Sr (> 228 ppm) suggest the rock was originated from the crust or there was a crust involvement during the generation of the rock. However, a relatively higher content of Y (> 16 ppm) also suggests another complex generation of the rock. High Al_2O_3 contents suggest high content of plagioclase phenocryst (Crawford, 1987, in Hartono, 1997). Foden and Varne (1981) argued that the crustal involvement was not possible because of the thinness of the crust in the area. However, considering the spider diagram pattern that shows a relatively similar pattern with those form upper crusts, it would be possible that a small amount of crustal involvement had occurred during the generation. It would be possible that a density filter or "host rock filter" occur during the magma ascending and caused the low Mg content in the melt.

Table 2. Normatif minerals of lava flows 1966 based on CIPW Norm Calculation Program

Normative Minerals	Sample Number							
	Lava 1966-1		Lava 1966-2		Lava 1966-5		Lava 1966-6	
	Weight % Norm	Volume % Norm	Weight % Norm	Volume % Norm	Weight % Norm	Volume % Norm	Weight % Norm	Volume % Norm
Quartz	7.81	8.49	6.41	7.03	6.74	7.36	10.63	11.44
Plagioclase	54.24	58.26	53.68	57.96	54.23	58.47	52.56	55.96
Orthoclase	11.52	12.98	10.87	12.34	10.87	12.31	13.77	15.34
Nepheline								
Leucite								
Kalsilite								
Corundum								
Diopside	11.75	10.06	15.06	12.95	13.22	11.36	10.71	9.04
Hypersthene	8.60	7.02	7.71	6.29	8.75	7.16	6.53	5.23
Wollastonite								
Olivine								
Larnite								
Acmite								
K_2SiO_3								
Na_2SiO_3								
Rutile								
Ilmenite	1.06	0.65	1.12	0.69	1.08	0.66	1.03	0.62
Magnetite	3.76	2.08	4.19	2.34	4.05	2.25	3.32	1.82
Hematite								
Apatite	0.51	0.46	0.44	0.40	0.46	0.42	0.63	0.56
Zircon								
Perovskite								
Chromite								
Sphene								
Pyrite								
Halite								
Fluorite								
Anhydrite								
Na_2SO_4								
Calcite								
Na_2CO_3								
Total	**99.25**	**100.00**	**99.48**	**100.00**	**99.40**	**99.99**	**99.18**	**100.01**

Conclusion

Based on the discussion above, it can be concluded that the Rombongan and Barujari lavas are composed of calc-alkaline and high K calc-alkaline porphyritic basaltic-andesite. Dominant phenocryst phases are plagioclase (andesine) and pyroxene (dominantly diopside and hypersthene). The magma shows a narrow variation of SiO_2 content that implies small changes. Magma that formed the Rombongan and Barujari lavas was an island-arc alkaline basalt. Generally, data show that the rocks are enriched in Large Ion Lithophile Elements

(LILE: K, Rb, Ba, Sr, and Ba) and depleted in High Field Strength Elements (HFSE: Y, Ti, and Nb) which is a typical suite of a subduction zone. The pattern shows a medium enrichment in Light REE and relatively depleted in Heavy REE.

The generation processes are dominantly controlled by fractional crystallization and magma mixing processes. All of the Barujari and Rombongan lavas would be produced by the same source of magma with little variation in composition caused by a host rock filter process. New input of magma would likely have occurred after the 1966 eruption indicated by the formation of relatively basic lava. The arc magma differentiation trend to the magnesian field leads to the formation of magnesian-end-member minerals.

Acknowledgements

The authors are grateful to Prof. Adjat Sudradjat, Ir. Oman Abdurahman, M.T., and Ir. R. Isnu H. Sulistyawan, M.T. for their critics and comments for this paper. The authors also thank Roni Permadi for his support to finish this paper.

References

Abbott, M.J. and Chamalaun, F.H., 1981. Geochronology of some Banda Arc volcanics. *The geology and tectonics of Eastern Indonesia,* 2, p.253-268.

Annen, C., Blundy, J.D., and Sparks, R.J.S., 2006. The genesis of intermediate and silicic magmas in deep crustal hot zones. *Journal of Petrology*, 47, p.505-539. DOI: 10.1093/petrology/egi084

Brouwer, H.A., 1942. *Summary of the geological results of the expedition*. NV Noord-Hollandsche Uitgevers Maatschappij. DOI: 10.1017/S0016756800082698

Curray, J.R., Shor, Jr., G.G., Raiit, R.W., and Henry, M., 1977. Seismic refraction and reflection studies of crustal structure of the eastern Sunda and western Banda arcs. *Journal of Geophysical Research*, 82, p.2479-2489. DOI: 10.1029/JB082i017p02479

Ehrat, H., 1928. Geologisch-mijnbouwkundige onderzoekingen op Flores. Jahrbook von het Mijnwerken, 1925. 2: 221-315. 1928b. Die Tiefengesteine der Kleinen Sunda Inseln. Neues Jahrbuch für *Geologie und Paläontologie Abhandlungen Abt. A*, 58, p.433-52.

Foden, J.D. and Varne, R., 1981. The Geochemistry and Petrology of Basalt-Andesite-Dacite Suite from Rinjani Volcano, Lombok: Implications for The Petrogenesis of Island Arc, Calcalkaline Magmas. The Geology and Tectonics of Eastem Indonesia, Geological Research and Development Centre. *Special Publication*, 2, p.115-134.

Frost, B.R. and Frost, C.D., 2014. *Essentials of Igneous and Metamorphic Petrology*. Cambridge University Press: New York, USA.

Hamilton, 1974. *Earthquake map of Indonesian region*. U.S. Geological Survey. Miscellaneous Investigation Serial Map 1-875-C, scale 1:5.000.000.

Haskim, L.A, Wildman, T.R., and Haskim, M.A., 1968. An accurate procedure for the determination of the rare earths by neutron activation. *Journal of Radioanalytical and Nuclear Chemistry*, 1, p.337-348. DOI: 10.1007/BF02513689

Hanson, G. N., 1980. Rare Earth Elements in Petrogenetic Studies of Igneous System. *Annual Review Earth and Planetary Science*, 8, p.371-406. DOI: 10.1146/annurev.ea.08.050180.002103

Hartono, U., 1997. Basaltic Andesite Resulted from A Reaction Between Hydrous Basaltic Magmas and Anhydrous Ferromagnesian Minerals : Evidence from The Lawu Volcano, Central Java. *Journal of Geological Resources*, VII (69), p.2-10.

Hatherton, T. and Dickinson, W.R., 1969. The relationship between andesitic volcanism and seismicity in Indonesia, the Lesser Antilles, and other island arcs. *Journal of Geophysical Research*, 74 (22), p.5301-5310. DOI: 10.1029/JB074i022p05301

Hutchison, C. S., 1976. Indonesian active volcanic arc: K, Sr, and Rb variation with depth to the Benioff zone. *Geology*, 4 (7), p.407-408. DOI: 10.1130/0091-7613(1976)4<407:IAVAKS>2.0.CO;2

Kusumadinata, K., Hadian, R., Hamidi, S., and Reksowirogo, L.D., 1979. *Data dasar gunungapi Indonesia*, Direktorat Vulkanologi, Dirjen Pertambangan Umum, Departemen Pertambangan dan Energi, Bandung.

Komorowski, J., Metrich, N., and Vidal, C., 2014. *Final Research Report for Ristek - 2013*. Institute de Physique Du Globe de Paris.

Lavigne, F., Degeai, J.P., Komorowski, J.C., Guillet, S., Robert, V., Lahitte, P., and Wassmer, P., 2013. Source of the great AD 1257 mystery eruption unveiled, Samalas volcano, Rinjani Volcanic Complex, Indonesia. *Proceedings of the National Academy of Sciences*, 110 (42), p.16742-16747. DOI: 10.1073/pnas.1307520110

Le Bass, 1985. Diagram TAS. *In*:Rollinson, H.R., 1993. *Using Geochemical Data: evaluation, presentation, interpretation*, John Willey & Sons Inc. New York, 50pp.

Le Bas, M.J., Le Maitre, R.W., Streckeisen, A., and Zanettin, B., 1986. A chemical classification of volcanic rocks based on the total alkali-silica diagram. *Journal of Petrology*, 27 (3), p.745-750. DOI: 10.1093/petrology/27.3.745

Mangga, S.A., Atmawinata, S., Hermanto, B., and Setyogroho, B., 1994. *Geological Map of The Lombok Sheet, West Nusa Tenggara, scale 1:250.000.* Geological Research and Development Centre, Bandung.

Manullang, S., Rosana, M.F., and Rachmat, H., 2015. Petrogenesa Batuan Lava Gunung Barujari dan Gunung Rombongan Komplek Gunung Rinjani. *Jurnal Gunungapi dan Mitigasi Bencana Geologi*, 7 (2), p.23-31. Pusat Vulkanologi dan Mitigasi Bencana Geologi, Bandung.

Matrais, I.B., 1972. *Hydrogeology of the Island of Lombok* (Indonesia).

Nakagawa, M., Takahashi, R., Amma-Miyasaka, M., Kuritani, T., Wibowo, H., Furukawa, R., and Takada, A., 2015. Petrology of Rinjani volcano, Indonesia: The magmatic processes before and during AD 1257 caldera-forming eruption. *Japan Geoscience Union Meeting*; 2015 May 24-28th: Makuhari Messe, Chiba.

Nasution, A., Takada, A., and Rosgandika, M., 2004. The volcanic activity of Rinjani, Lombok Island, Indonesia, during the last thousand years, viewed from 14C datings; Abstract. *The 33rd Annual Convention & Exhibition, IAGI*, 29 Nov-1 Oct 2004, Bandung, Indonesia.

Nasution, A., Takada, A., Udibowo, Widarto, D., and Hutasoit, L., 2010. Rinjani and Propok Volcanics as a Heat Sources of Geothermal Prospect from Eastern Lombok, Indonesia. *Jurnal Geoaplika*, 5 (1), p.001-009.

Neumann van Padang, M., 1951. Indonesia: Catalogue of active volcanoes of the world. *IAVCEI*, 1, p.1-271.

Nixon G.T. and Pearce T.H., 1987. Laser-interferometry study of oscillatory zoning in plagioclase: the record of magma mixing and phenocryst recycling in calc-alkaline magma chambers, Iztaccihuatl volcano, Mexico. *American Mineralogist*, 72, p.1144-1162.

Peccerillo, R. and Taylor, S.R., 1976. Geochemistry of Eocene calc-alkaline volcanic rocks from the Kastamonu area, northen Turkey. *Contribution to Mineralogy and Petrology*, 56, p.221-246. DOI: 10.1007/BF00384745

Rachmat, H. and Iqbal, M., 2000. *Gunungapi Nusa Tenggara Barat*. Kanwil DESDM Propinsi NTB.

Rachmat, H., 2016. Rinjani Dari Evolusi Kaldera Hingga Geopark. *Majalah Geomagz*, 6 (1), p.28-33.

Rollinson, H., 1993. *Using geochemical data: Evaluation, presentation, interpretation.* Essex, UK: Addison Wesley, Longman Ltd.

Sigl, M., McConnell, J.R., Toohey, M., Curran, M., Das, S.B., Edwards, R., Isaksson, E., Kawamura, K., Kipfstuhl, S., Krueger, K., Layman, L., Maselli, O.J., Motizuki, Y., Motoyama, H., Pasteris, D.R., and Se-

veri, M., 2014. Insights from Antarctica on volcanic forcing during the Common Era. *Nature Climate Change*, 4, p.693-697. DOI: 10.1038/nclimate2293

Sigl, M., Winstrup, M., McConnell, J. R., Welten, K.C., Plunkett, G., Ludlow, F., Büntgen, U., Caffee, M.W., Chellman, N. J., Dahl-Jensen, D., Fischer, H., Kipfstuhl, S., Kostick, C., Maselli, O.J., Mekhaldi, F., Mulvaney, R., Muscheler, R., Pasteris, D.R., Pilcher, J.R., Salzer, M., Schüpbach, S., Steffensen, J.P., Vinther, B., and Woodruff, T.E., 2015. Timing and climate forcing of volcanic eruptions for the past 2,500 years. *Nature*, 523, p.543-549. DOI: 10.1038/nature14565

van Bemmelen, R.V., 1949. The geology of Indonesia, vol. IA, *General Geology of Indonesia and Adjacent Archipelagoes*, Martinus Nijhoff, The Hague, Netherlands, 732pp.

Vidal, C.M., Komorowski, J., Métrich, N., Pratomo, I., Kartadinata, N., Prambada, O., Michel, A., Carazzo, G., Lavigne, F., Rodysill, J., Fontijn, K., and Surono, 2015. Dynamic of the major plinian eruption of Samalas in 1257 A.D. (Lombok, Indonesia). *Bulletin Volcanol*ogy (2015) 77:73: Springer-Verlag Berlin Heidelberg. DOI: 10.1007/s00445-015-0960-9

Whitford, D. J., Compston, W., Nicholls, I. A., and Abbott, M. J., 1977. Geochemistry of late Cenozoic lavas from eastern Indonesia: Role of subducted sediments in petrogenesis. *Geology*, 5(9), p.571-575. DOI: 10.1130/0091-7613(1977)5<571:GOLCLF>2.0.CO;2